Monothiolation and Reduction of Graphene Oxide *via* One-Pot Synthesis: Hybrid Catalyst for Oxygen Reduction

Chun Kiang Chua and Martin Pumera*

Division of Chemistry and Biological Chemistry, School of Physical and Mathematical Sciences, Nanyang Technological University, Singapore 637371, Singapore

ABSTRACT The functionalization of graphene provides diverse possibilities to improve the handling of graphene and enable further chemical transformation on graphene. Graphene functionalized with mainly heteroatom-based functional groups to enhance its chemical and physical properties is intensively pursued but often resulted in grafting of the heteroatoms as various functional groups. Here, we show that graphene oxide can be functionalized with predominantly a single type of sulfur moiety and reduced simultaneously to form monothiol-functionalized graphene. The thiol-functionalized graphene shows a high electrical conductivity and heterogeneous electron transfer rate. Graphene is also embedded with a trace amount of manganese impurities originating from a prior graphite oxidation process, which facilitates the thiol-functionalized graphene to function as a hybrid electrocatalyst for oxygen reduction reactions in alkaline medium with an onset potential lower than for Pt/C. Further characterizations of the graphene are performed with X-ray photoelectron spectroscopy, scanning electron microscopy with energy-dispersive X-ray spectroscopy, Fourier transform infrared spectroscopy, thermogravimetric analysis, Raman spectroscopy, and electrochemical impedance spectroscopy. This material contributes to the class of hybrids that are highly active electrocatalysts.

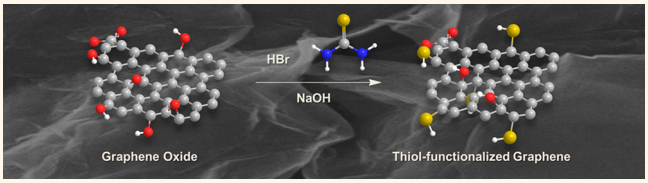

KEYWORDS: graphene · hybrid materials · catalysis · chemical functionalization · electrochemistry

The successful isolation of graphene, an atom-thick two-dimensional (2D) planar sheet of sp^2-hybridized carbon, has initiated a rapid development of 2D nanomaterials.[1−3] The planar structure of graphene confers numerous unique physical, electrical, and electronic properties that are suitable for applications in high-performance electronics, energy storage and generation devices, and biological and chemical sensors.[4,5]

Despite such positive outlooks on graphene, the direct application of graphene is greatly hampered by its low solubility in both aqueous and organic solvents as well as its intrinsic zero band gap energy. Efforts to improve the handling of graphene without compromising its unique properties have led to the development of chemically modified graphene (CMGs) materials, which include graphite oxide, graphene oxide, and reduced (thermally, chemically, electrochemically) graphene oxide.[6] Chemical functionalizations/modifications are frequently performed on CMGs to further improve their chemical, electrical, and physical properties, for example, by introducing new functional groups that can function as anchor points for further chemical alterations.[7,8]

The functionalization of CMGs with predominantly heteroatom-based functional groups has gained much attention given their enhanced performances as electrocatalysts for oxygen reduction reactions[9] and as materials for supercapacitors[10] in recent years. Chemical functionalization should be contrasted with chemical doping, whereby the former involves the covalent attachment of functional groups, while the latter involves the replacement of an element from the crystal lattice of the material. In the case of doping, CMGs are frequently doped with sulfur, nitrogen, phosphorus, and boron by thermal exfoliation and hydrothermal and solvothermal methods.[11−13] However, most of these techniques suffer

* Address correspondence to pumera.research@gmail.com.

Received for review January 20, 2015 and accepted March 24, 2015.

Published online March 27, 2015
10.1021/acsnano.5b00438

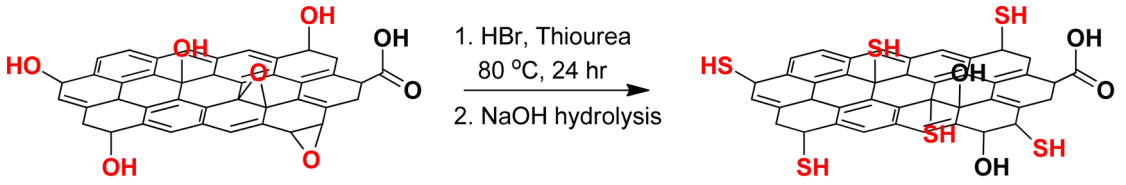

Graphene Oxide (GO) Thiol-functionalized Graphene (G-SH)

Figure 1. Functionalization of GO with a thiol group to provide G-SH.

from heterogeneity of functional groups in the produced CMGs due to the lack of control and knowledge on the underlying reaction mechanisms occurring during the high-temperature and/or -pressure processes. The resulting CMGs usually contain a mixture of doped and functionalized sites. For example, nitrogen-functionalized graphene synthesized by the hydrothermal method is usually decorated with a mixture of pyridinic, pyrrolic, amino, and quaternary nitrogen moieties.[14,15] In the case of sulfur modification at high temperatures, thiols, $-SO_3$, sulfur-epoxy, and thiophene-like moieties are introduced into the graphene backbone.[16,17] The presence of unintended chemical moieties can unfortunately affect the properties and performances of the CMGs.

In the case of chemical functionalization, the introduction of new functional groups can deliver new materials for modern applications. Moreover, chemical functionalization by the wet chemistry method can provide precise modifications with known synthetic mechanisms.[8] In fact, the wet chemistry method is a convenient approach since the reaction conditions can be easily controlled and manipulated to specifically target a certain functional group transformation on graphene.

While amine-functionalized CMGs are widely pursued, the synthesis of sulfur-functionalized CMGs by the wet chemistry method lacks investigations. In this case, we specifically refer only to functionalization in which the nitrogen and sulfur elements are covalently attached to the carbon lattice of CMGs. Rourke and co-workers have recently functionalized graphene oxide with sulfur *via* epoxide ring-opening.[18] The resulting thiol-saturated graphene oxide was subsequently applied as a nucleophile to synthesize thioether-functionalized graphene oxide. This is, to the best of our knowledge, the only report on well-targeted sulfur functionalization on graphene oxide.

Herein, we propose a one-pot monothiolation and reduction of graphene oxide to provide thiol-functionalized graphene (Figure 1). In this strategy, hydroxyl and epoxide groups were targeted for thiolation. This is achieved by first subjecting graphene oxide to hydrobromic acid to achieve simultaneous reduction and bromination effects on graphene oxide. Subsequent addition of thiourea followed by hydrolysis with sodium hydroxide gave thiol-functionalized graphene (G-SH). Base-washed graphene oxide (GO) was used to avoid possible side reactions with oxidation debris resulting from the earlier oxidation process.[19] Moreover, rigorous washing steps including alternate vacuum filtration and ultrasonication treatments were followed to remove potentially adsorbed thiourea. The resulting G-SH has been characterized for its structural, electrical, and electrochemical properties with X-ray photoelectron spectroscopy (XPS), scanning electron microscopy with energy-dispersive X-ray spectroscopy (SEM-EDX), Fourier transform infrared spectroscopy (FTIR), thermogravimetric analysis (TGA), Raman spectroscopy, electrochemical impedance spectroscopy (EIS), cyclic voltammetry, and electrical conductivity analyses.

The structural, electrical, and electrochemical properties of GO and G-SH were compared side-by-side to elucidate the success of the functionalization. Subsequently, the capability of G-SH containing a small amount of manganese for oxygen reduction reaction was examined to highlight its potential as a promising hybrid electrocatalyst toward oxygen reduction reaction (ORR) in alkaline medium.

RESULTS AND DISCUSSION

The monothiolated graphene was synthesized from base-washed graphene oxide *via* a one-pot reaction. The GO suspension was initially treated with hydrobromic acid, which resulted in nucleophilic substitution and addition reactions on hydroxyl and epoxide groups, respectively. Simultaneous high-temperature treatment resulted in dehydration and partial dehydrobromination events, which provided highly brominated chemically reduced graphene. Following that, the addition of thiourea containing a nucleophilic sulfur center reacted with the bromine moieties to form isothiouronium salts, which were subsequently hydrolyzed by base treatment to result in thiol-functionalized graphene (Scheme S1, Supporting Information). The obtained G-SH was well characterized as below.

Structural Characterization. The success of the thiol functionalization method was strongly supported by X-ray photoelectron spectroscopy. XPS survey scans provide an overall outlook on the surface elemental composition of the graphene materials. The survey scan of GO in Figure 2A showed 72.01 at. % carbon and 27.99 at. % oxygen. On the other hand, G-SH consisted of 82.32 at. % carbon, 15.05 at. % oxygen,

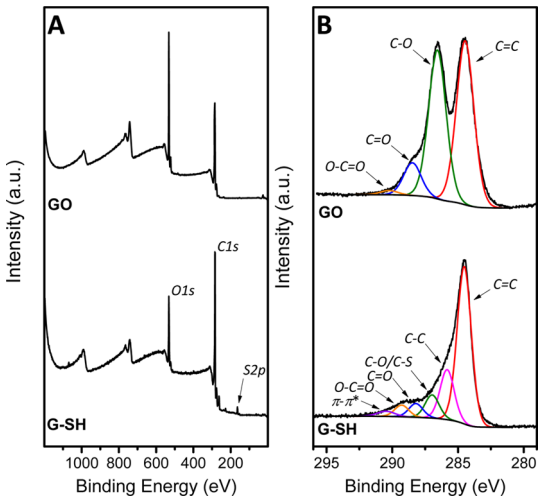

Figure 2. XPS spectra of (A) survey and (B) C 1s core level for GO and G-SH.

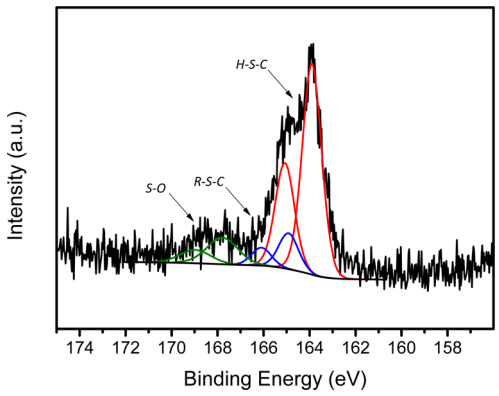

Figure 3. S 2p core-level spectrum of G-SH.

2.10 at. % sulfur, and 0.53 at. % nitrogen. As the presence of nitrogen may signify potentially adsorbed or unhydrolyzed thiourea in G-SH, the actual amount of sulfur could be lower, at 1.84 at. %. The presence of sulfur in the survey scan was an early indication for the success of the functionalization. The extent of the functionalization is directly influenced by the extent of bromination in the initial treatment of GO with hydrobromic acid.[20,21] The likelihood of thiol dissociating from the surface of graphene could also result in the low percentage of sulfur.[22] However, the presence of oxygen-containing groups may help to stabilize the remaining thiol groups by weak interactions such as intramolecular hydrogen bonding. Apart from that, the carbon to oxygen atomic ratios for GO and G-SH were 2.57 and 5.47, respectively. The higher C/O ratio of G-SH suggested an effective reduction process during the functionalization treatment. In fact, this also reflected the success of the bromination step, which included epoxide ring-opening and nucleophilic substitution on hydroxyl groups.

These changes can be observed more clearly in the high-resolution C 1s core-level spectra, as shown in Figure 2B. A typical C 1s core-level spectrum can be deconvoluted into several peaks including C═C (∼284.5 eV), C−C (∼285.6 eV), C−O/C−S (∼286.6 eV), C═O (∼288.2 eV), O−C═O (∼289.2 eV), and $\pi-\pi^*$ (∼290.4 eV). A drastic decrease in the peak intensity of C−O was observed from the conversion of GO to G-SH. As aforementioned, this could arise from the epoxide ring-opening and nucleophilic substitution of hydroxyl groups by bromine.

On top of that, a sharper and well-defined C═C signal in conjunction with the presence of a $\pi-\pi^*$ shake up satellite band on G-SH signified an improved characteristic of conjugated/aromatic systems. This resulted from the bromination treatment, which reduced GO to graphene. The substantial presence of O−C═O on G-SH reflected the availability of carboxyl groups, which helped to disperse G-SH in DMF for more than two months. Apart from that, since the binding energy of the C−S bond was indistinguishable from the C−O bond in the C 1s core-level spectrum, a high-resolution S 2p core-level spectrum was obtained to provide more details on the nature of the chemical bonding types for sulfur (Figure 3).

The core-level spectrum of S 2p was split into spin−orbit doublets of S $2p_{3/2}$ and S $2p_{1/2}$ (with a typical splitting magnitude of 1.18 eV). In particular, three S $2p_{3/2}$ peaks were observed, representing sulfur bonding of H−S−C (∼163.5 eV), R−S−C (∼164.5 eV), and S−O (∼168.0 eV). The largest peak arising from the H−S−C bond indicated a successful grafting of predominantly thiol groups onto the graphene carbon lattice. The R−S−C peak could arise from a small presence of unhydrolyzed thiourea, while the S−O peak could be due to unwanted oxidation byproducts.

In addition to the XPS measurements, EDX analyses on G-SH highlighted the presence of sulfur at 3.9 at. % (Figure S1A, Supporting Information). The EDX spectrum also showed peaks corresponding to oxygen and sodium at 10.8 and 1.0 at. %, respectively. The minor amount of sodium was a result of base treatment (sodium hydroxide) from both the production step of base-washed graphite oxide and the hydrolysis step of the isothiouronium salt. The EDX analyses also showed a homogeneous distribution of sulfur on G-SH (Figure 4C−F). More importantly, sulfur was not observed in the EDX spectrum of GO (Figures S1B and S2C−E, Supporting Information). The SEM images of G-SH at magnifications of 60 000× and 10 000× showed exfoliated nonagglomerated graphene sheets that are highly wrinkled and wave-like (Figure 4A,B). In contrast, the SEM images of GO revealed stacked and crumpled graphene sheets (Figure S2A,B, Supporting Information).

Subsequent FTIR analyses of GO and G-SH were performed to detect the evolution of a S−H vibrational band at ∼2400−2500 cm^{-1}. Typical FTIR peaks corresponding to an O−H stretching band (∼3200 cm^{-1}), C−OH vibrational mode (∼1380 and 1050 cm^{-1}), C═O

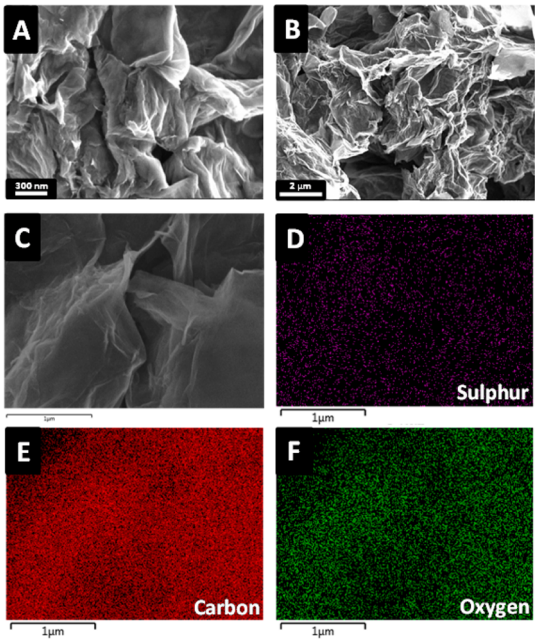

Figure 4. SEM images of G-SH at (A) 60 000× and (B) 10 000×. EDX analyses of G-SH on the electron image (C) with mapping of (D) sulfur, (E) carbon, and (F) oxygen elements.

vibrational mode (~1718 cm^{-1}), epoxide bending and stretching modes (~870 and 1250 cm^{-1}), and a water bending mode (~1600 cm^{-1}) were observed on the GO spectrum (Figure S3A, Supporting Information). However, the bromination and thiolation treatment on GO resulted in the disappearance of most carbon−oxygen modes except that of the C═O vibration mode, which was still visible at ~1718 cm^{-1} on the FTIR spectrum of G-SH. The anticipated S−H vibrational band was not obvious despite the earlier XPS and EDX analyses, likely due to the inherent weak vibration mode of the S−H bond and the low amount of S−H at ~1.84 at. %. This observation was not an isolated case, as an earlier work on sulfur-functionalized graphene was unsuccessful in detecting the S−H peak by FTIR spectroscopy as well.[18]

Thermogravimetric analysis was performed to analyze the thermal stability of GO and G-SH (Figure S3B, Supporting Information). The measurements were performed at a heating rate of 5 °C min^{-1} under a nitrogen atmosphere. GO showed weight loss over two intervals, at (i) 25−100 °C with 18 wt % loss due to the elimination of interlamellar water and (ii) 100−200 °C with 23 wt % loss due to removal of oxygen-containing groups from the GO sheets. G-SH was comparably more thermally stable and less hygroscopic than GO, as only 9 wt % loss was observed at 200 °C.

Further analyses with Raman spectroscopy on GO and G-SH showed obvious D (breathing mode of sp^2-hybridized carbon) and G (graphitic sp^2-hybridized carbon) bands, as seen in Figure 5. The ratio of peak intensities for D and G bands (I_D/I_G) reflects the extent

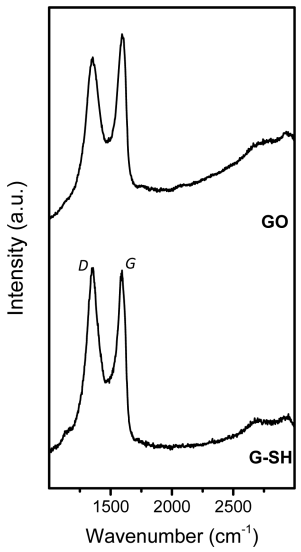

Figure 5. Raman spectra of GO and G-SH.

of defects on graphene materials, in which GO and G-SH showed values of 0.83 and 0.94, respectively. This also corresponded to changes of the average crystalline size from 20.1 nm to 17.9 nm upon functionalization treatment. The slightly higher extent of defects on G-SH is common for GO materials that have undergone reduction or functionalization treatments.[23] However, the smaller full-width half-maximum value of the D band on G-SH indicated a lesser extent of structural disorder including sp^3-hybridized and short-range sp^2-hybridized carbon moieties.[24] Moreover, a red shift (~10 cm^{-1}) observed on the G band of G-SH also suggested an increasing proportion of C═C bond type in it.[24,25]

Electrical and Electrochemical Characterizations. The success of the thiol functionalization as determined by the structural characterization above prompted further examination on its electrical and electrochemical performances. As such, electrical conductivity measurements, cyclic voltammetry analyses, and electrochemical impedance spectroscopy were performed.

The electrical conductivity of GO and G-SH was measured using an interdigitated gold electrode (Au-IDE) platform coupled with the linear sweep voltammetry technique as shown in Figure 6A. Materials with "ohmic" behaviors would provide linear $I-V$ curves with slopes directly proportional to their conductivities.[26] A steep slope was observed on G-SH (55.9 mA V^{-1}), while GO showed almost zero current. This indicated the insulator-semiconducting properties of GO. The slope of G-SH exceeded even that of graphene oxide treated with hydrobromic acid at high temperature (39 mA V^{-1}).[20] In comparison to G-SH, hydrazine-reduced graphene (concurrently N-doped) produced from similar types of graphite and an oxidation procedure registered only 8.6 mA V^{-1}.[23] Such enhanced electrical conductivity was likely due to an

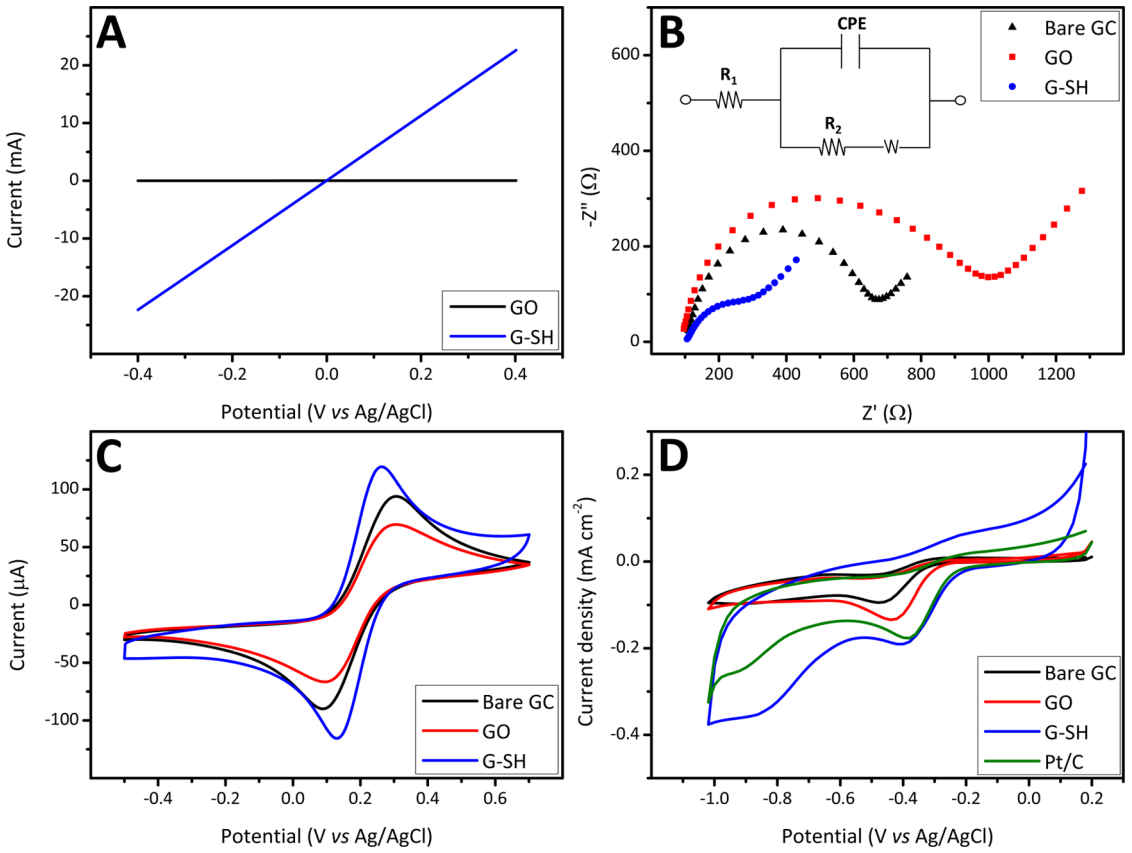

Figure 6. (A) Current−voltage curves of GO and G-SH for electrical conductivity analyses. (B) Nyquist plots for EIS measurements of bare GC, GO, and G-SH. Conditions: PBS (50 mM) background electrolyte at pH 7.4, 10 mM $K_3[Fe(CN)_6]$/$K_4[Fe(CN)_6]$, scan rate of 100 mV s^{-1}. The Randles equivalent circuit was used for data fitting as shown in the inset. (C) Cyclic voltammograms of bare GC, GO, and G-SH. Conditions: PBS (50 mM) background electrolyte at pH 7.4, 10 mM $K_3[Fe(CN)_6]$/$K_4[Fe(CN)_6]$, scan rate of 100 mV s^{-1}. (D) Cyclic voltammograms of bare GC, GO, G-SH, and Pt/C for ORR activities analyses. Conditions: 0.1 M KOH solution, pH 12.9, scan rate of 100 mV s^{-1}.

improved regeneration of an sp^2 carbon network and a lower electronegativity of sulfur as compared to nitrogen.

Subsequently, electrochemical impedance spectroscopy and cyclic voltammetry analyses were carried out to probe the resistance of GO and G-SH toward heterogeneous charge transfer. EIS is a technique that applies small alternating-current voltage perturbation (on the order of millivolts) to a system at different frequencies, while cyclic voltammetry complements the technique by applying a large perturbation (on the order of hundreds of millivolts) to the system. In general, the surface morphologies of graphene materials affect the ability of the materials to transfer and exchange charges with surrounding molecules. By using ferro/ferricyanide as an electrochemical probe, cyclic voltammetry and EIS analyses were performed. Nyquist plots obtained from the EIS measurements were analyzed by fitting with a Randles equivalent circuit (Figure 6B). The diameter of the semicircle Nyquist plot corresponds to the charge transfer resistance (R_{ct}) of the material. The bare GC electrode showed a R_{ct} of 580 Ω, while the highly oxidized GO gave a higher R_{ct} of 810 Ω. The increase in R_{ct} is common for graphene materials with oxygen-containing groups and is due to the electrostatic repulsion between both the negatively charged oxygen-containing groups (at pH 7.4) and the ferro/ferricyanide complexes.[27] Following the functionalization treatment, G-SH exhibited a 4-fold decrease in R_{ct}, at 170 Ω. This signified the diminishing amount of oxygen-containing groups, as also highlighted by the XPS and SEM-EDX analyses, and its suitability for use as an electrode material.

Further cyclic voltammetry analyses were performed to examine the heterogeneous electron transfer (HET) rate of the graphene materials based on Nicholson's[28] method. Similar to EIS, an increasing amount of oxygen-containing groups on the graphene materials can decrease the HET rate (reflected by an increase of peak-to-peak separation, ΔE). The cyclic voltammograms of bare GC, GO, and G-SH shown in Figure 6C measured ΔE values of 213, 201, and 134 mV (*vs* Ag/AgCl), respectively. This corresponded to HET (k^o_{obs}) rates of 9.22×10^{-4}, 1.07×10^{-3}, and 2.69×10^{-3} cm s^{-1}, respectively. Although the measured value for GO was very similar to that of bare GC, its lower peak current shows a lower amount of available ferro/ferricyanide electrochemical probe due to

electrostatic repulsion. Nevertheless, the high HET rate registered by G-SH suggested a lower presence of oxygen-containing groups on its surface.

Oxygen Reduction Reaction. GO and G-SH were further examined for their electrocatalytic properties for oxygen reduction reaction in an alkaline medium by performing cyclic voltammetry scans in a 0.1 M KOH solution. The performance of G-SH was compared with bare GC and Pt/C. As observed in Figure 6D, distinct cathodic peaks corresponding to ORR activities can be observed from all the materials (see Figure S4 for scans in N_2-saturated solution, Supporting Information). Bare GC, GO, and Pt/C registered ORR peak potentials at −479, −446, and −380 mV (*vs* Ag/AgCl). Upon thiolation, G-SH showed a more negative peak potential at −403 mV, as compared to GO. Further analyses on G-SH indicated that it has a higher current density and a lower onset potential than Pt/C. The onset potential observed on G-SH was −190 mV. This differed by about 20 mV from that of Pt/C, which was −211 mV. In comparison, the onset potentials of bare GC and GO were −300 and −292 mV, respectively.

In view of the recent report on the influence of MnO_2 impurities on the electrocatalytic capability of chemically reduced graphene materials toward ORR,[29] additional investigations were performed on GO and G-SH materials. On the basis of ICP-MS measurements, GO and G-SH contained about 600 ppm of manganese (Table S1, Supporting Information). Cyclic voltammograms of MnO_2 measured in alkaline medium showed a peak potential and onset potential of −465 and −212 mV, respectively (Figure S5, Supporting Information). It is clear that G-SH in conjunction with trace Mn-based impurities/dopants acts as a highly active hybrid electrocatalyst showing a lower overpotential and higher current density toward ORR than commercially available Pt/C.

CONCLUSION

In summary, thiol-functionalized graphene has been produced *via* a one-pot functionalization and reduction of graphene oxide. The structural characterizations based on XPS, SEM-EDX, and Raman spectroscopy indicated a successful functionalization process. The resulting thiol-functionalized graphene contained almost only −SH groups with 1.84 at. % sulfur based on XPS analysis and remained as stable suspensions in DMF. G-SH also demonstrated a higher electrical conductivity and heterogeneous electron transfer rate in comparison to GO. Moreover, G-SH together with residual Mn-based impurities functioned as a hybrid electrocatalyst to promote oxygen reduction reaction with an onset potential at 45 mV, which is rivaling the commercial Pt/C catalyst. The success of this method provides a simple and scalable one-pot synthesis of thiol-functionalized graphene to facilitate future developments of advanced graphene-based applications. It could notably be useful for the conjugation of biomolecules *via* sulfhydryl−maleimide interaction and for the adsorption of metal nanoparticles.

EXPERIMENTAL SECTION

Materials. Natural graphite was obtained from Asbury Carbons, USA. Sulfuric acid (95−98%), hydrochloric acid (37%), sodium hydroxide, sodium nitrate, manganese(IV) oxide (99.997%), and Pt/C (20 wt %) were purchased from Sigma-Aldrich, Singapore. Hydrogen peroxide and hydrobromic acid (48%) were obtained from Alfa Aesar, Singapore. Thiourea (96%) was obtained from Samchun Chemicals. Potassium permanganate was obtained from J.T. Baker. Milli-Q water (resistivity: 18.2 MΩ·cm) was used throughout the experiments.

Apparatus. X-ray photoelectron spectroscopy was performed with a Phoibos 100 spectrometer and Mg X-ray radiation source (SPECS, Germany). Both survey and high-resolution spectra for C 1s, O 1s, and S 2p were collected. Relative sensitivity factors were used for evaluation of atomic percentage from the XPS survey spectra measurements. XPS samples were prepared by coating a carbon tape with a uniform layer of the materials under study. Attenuated total reflectance Fourier transform infrared measurements were carried out on a Perkin-Elmer Spectrum 100 system coupled with a universal ATR accessory. A diamond/ZnSe was used as the ATR crystal. Thermogravimetric analyses were performed on a Q500 (TA Instruments, USA) by heating the material from room temperature to 800 °C at 5 °C min^{-1} in the presence of nitrogen flow at 60 mL min^{-1}. Raman spectroscopy analysis was performed using a confocal micro-Raman LabRam HR instrument from Horiba Scientific in backscattering geometry with a CCD detector, a 514.5 nm Ar laser, and a 100× objective mounted on an Olympus optical microscope. The calibration is initially made using an internal silicon reference at 520 cm^{-1} and gives a peak position resolution of less than 1 cm^{-1}. The spectra are measured from 1000 to 3000 cm^{-1}. A JEOL JSM-7600F semi-in-lens FE-SEM was used to acquire the SEM and STEM images. The solid samples were transferred to a carbon tape held onto a SEM holder for analyses. EDX data were obtained using an Oxford instrument and analyzed using Aztec software. Elemental analyses were performed using an Agilent model 7700x ICP-MS, and microwave digestions with concentrated nitric acid were performed on a Mars CEM system. All voltammetric experiments were performed on a μAutolab type III electrochemical analyzer (Eco Chemie, The Netherlands) connected to a personal computer and controlled by General Purpose Electrochemical Systems version 4.9 software (Eco Chemie).

Procedures. *Base-Washed Graphite Oxide.* Graphite oxide was prepared by the modified Hummers method.[30] Graphite (0.5 g) was stirred with 23.0 mL of sulfuric acid (95−98%) for 20 min at 0 °C prior to the addition of $NaNO_3$ (0.5 g) in portions. The mixture was left to stir for 1 h. $KMnO_4$ (3 g) was then added in portions at 0 °C. The mixture was subsequently heated to 35 °C for 1 h. Water (40 mL) was then added into the mixture and resulted in the temperature of the mixture rising to 90 °C. The temperature was maintained at 90 °C for 30 min. Additional water (100 mL) was added into the mixture. This was followed by a slow addition of 30% H_2O_2 (∼10 mL). The warm solution was centrifuged and washed with warm water (100 mL). The solid was subsequently washed with a copious amount of water until a neutral pH was obtained. The materials were kept in a vacuum oven at 30 °C for 5 days prior to washing with base. To a graphite oxide dispersion in water was added NaOH under constant stirring to give a 14 mM solution. The mixture was heated to 70 °C for 1 h. The obtained dark brown solution was centrifuged (12 500 rpm, 30 min) to obtain a dark brown pellet.

The pellet was redispersed and washed with water before the addition of HCl to form a 14 mM solution. The mixture was stirred at 70 °C for 1 h. The mixture was centrifuged and washed with water six times before the pellet was collected and dried in a vacuum oven at 30 °C for 5 days to provide GO.

Thiol Functionalization. GO (15 mg) was dispersed in water to form a 1 mg/mL dispersion after ultrasonication treatment for 1 h. HBr (1 mL) was added, and the mixture was stirred at 30 °C for 2 h. Thiourea (1 g) was subsequently added and stirred at 80 °C for 24 h. The solution was cooled to room temperature before addition of 4 M NaOH (10 mL). The mixture was stirred at room temperature for 30 min. The mixture was then filtered and washed with ether and water over a 0.2 μm PTFE membrane. The filtered solid was redispersed in water and ultrasonicated for 5 min three times. The collected solid was stored in a vacuum oven at 30 °C for 5 days to provide G-SH.

Electrochemical Measurements. The electrochemical experiments were carried out in a 10 mL voltammetric cell at room temperature using a three-electrode configuration. A platinum electrode served as an auxiliary electrode and a Ag/AgCl electrode as a reference electrode; a glassy carbon electrode was utilized as a working electrode. Prior to a measurement, the glassy carbon electrode was polished with 0.05 μm alumina on a polishing cloth. The working electrode was then modified by applying 1 μL of 1 mg/mL materials dispersed in DMF and allowed to dry. Onset potential of ORR measurements were determined as the potential at 10% of the wave current.

Electrical Conductivity Measurements. Current−voltage measurements ($I-V$ curve) were conducted with an interdigitated gold electrode platform by depositing 2 μL of the material suspension (prepared at 1 mg/mL concentration in water) onto the electrode surface with 10 μm spacing. The electrode was then dried under a lamp for 20 min, leaving a randomly deposited material film on the interdigitated area bridging the two Au electrode bands. The $I-V$ curves were obtained by linear sweep voltammetric measurements at a 20 mV s^{-1} scan rate. A Au band measured 175 mA V^{-1}. The displayed data correspond to the average from three measurements.

Conflict of Interest: The authors declare no competing financial interest.

Supporting Information Available: Additional EDX, SEM, FTIR, TGA, ICP-MS, and ORR analysis data and reaction schemes are included. This material is available free of charge *via* the Internet at http://pubs.acs.org.

Acknowledgment. M.P. acknowledges a Tier 2 grant (MOE2013-T2-1-056; ARC 35/13) from the Ministry of Education, Singapore.

REFERENCES AND NOTES

1. Novoselov, K. S.; Fal'ko, V. I.; Colombo, L.; Gellert, P. R.; Schwab, M. G.; Kim, K. A Roadmap for Graphene. *Nature* **2012**, *490*, 192–200.
2. Geim, A. K.; Grigorieva, I. V. Van der Waals Heterostructures. *Nature* **2013**, *499*, 419–425.
3. Novoselov, K. S.; Geim, A. K.; Morozov, S. V.; Jiang, D.; Zhang, Y.; Dubonos, S. V.; Grigorieva, I. V.; Firsov, A. A. Electric Field Effect in Atomically Thin Carbon Films. *Science* **2004**, *306*, 666–669.
4. Geim, A. K.; Novoselov, K. S. The Rise of Graphene. *Nat. Mater.* **2007**, *6*, 183–191.
5. Geim, A. K. Graphene: Status and Prospects. *Science* **2009**, *324*, 1530–1534.
6. Dreyer, D. R.; Park, S.; Bielawski, C. W.; Ruoff, R. S. The Chemistry of Graphene Oxide. *Chem. Soc. Rev.* **2010**, *39*, 228–240.
7. Georgakilas, V.; Otyepka, M.; Bourlinos, A. B.; Chandra, V.; Kim, N.; Kemp, K. C.; Hobza, P.; Zboril, R.; Kim, K. S. Functionalization of Graphene: Covalent and Non-Covalent Approaches, Derivatives and Applications. *Chem. Rev.* **2012**, *112*, 6156–6214.
8. Chua, C. K.; Pumera, M. Covalent Chemistry on Graphene. *Chem. Soc. Rev.* **2013**, *42*, 3222–3233.
9. Ambrosi, A.; Chua, C. K.; Bonanni, A.; Pumera, M. Electrochemistry of Graphene and Related Materials. *Chem. Rev.* **2014**, *114*, 7150–7188.
10. Lai, L. F.; Chen, L. W.; Zhan, D.; Sun, L.; Liu, J. P.; Lim, S. H.; Poh, C. K.; Shen, Z. X.; Lin, J. Y. One-Step Synthesis of NH_2-Graphene from *in Situ* Graphene-Oxide Reduction and Its Improved Electrochemical Properties. *Carbon* **2011**, *49*, 3250–3257.
11. Liu, H.; Liu, Y.; Zhu, D. Chemical Doping of Graphene. *J. Mater. Chem.* **2011**, *21*, 3335–3345.
12. Wang, X.; Sun, G.; Routh, P.; Kim, D. H.; Huang, W.; Chen, P. Heteroatom-Doped Graphene Materials: Syntheses, Properties and Applications. *Chem. Soc. Rev.* **2014**, *43*, 7067–7098.
13. Kong, X. K.; Chen, C. L.; Chen, Q. W. Doped Graphene for Metal-Free Catalysis. *Chem. Soc. Rev.* **2014**, *43*, 2841–2857.
14. Yang, S. B.; Zhi, L. J.; Tang, K.; Feng, X. L.; Maier, J.; Mullen, K. Efficient Synthesis of Heteroatom (N or S)-Doped Graphene Based on Ultrathin Graphene Oxide-Porous Silica Sheets for Oxygen Reduction Reactions. *Adv. Funct. Mater.* **2012**, *22*, 3634–3640.
15. Jiang, Z. Q.; Jiang, Z. J.; Tian, X. N.; Chen, W. H. Amine-Functionalized Holey Graphene as a Highly Active Metal-Free Catalyst for the Oxygen Reduction Reaction. *J. Mater. Chem. A* **2014**, *2*, 441–450.
16. Yang, Z.; Yao, Z.; Li, G.; Fang, G.; Nie, H.; Liu, Z.; Zhou, X.; Chen, X. a.; Huang, S. Sulfur-Doped Graphene as an Efficient Metal-Free Cathode Catalyst for Oxygen Reduction. *ACS Nano* **2011**, *6*, 205–211.
17. Poh, H. L.; Šimek, P.; Sofer, Z.; Pumera, M. Sulfur-Doped Graphene *via* Thermal Exfoliation of Graphite Oxide in H_2S, SO_2, or CS_2 Gas. *ACS Nano* **2013**, *7*, 5262–5272.
18. Thomas, H. R.; Marsden, A. J.; Walker, M.; Wilson, N. R.; Rourke, J. P. Sulfur-Functionalized Graphene Oxide by Epoxide Ring-Opening. *Angew. Chem., Int. Ed.* **2014**, *53*, 7613–7618.
19. Rourke, J. P.; Pandey, P. A.; Moore, J. J.; Bates, M.; Kinloch, I. A.; Young, R. J.; Wilson, N. R. The Real Graphene Oxide Revealed: Stripping the Oxidative Debris from the Graphene-like Sheets. *Angew. Chem.* **2011**, *123*, 3231–3235.
20. Chua, C. K.; Pumera, M. Renewal of sp^2 Bonds in Graphene Oxides *via* Dehydrobromination. *J. Mater. Chem.* **2012**, *22*, 23227–23231.
21. Chen, Y.; Zhang, X.; Zhang, D.; Yu, P.; Ma, Y. High Performance Supercapacitors Based on Reduced Graphene Oxide in Aqueous and Ionic Liquid Electrolytes. *Carbon* **2011**, *49*, 573–580.
22. Denis, P. A. Density Functional Investigation of Thioepoxidated and Thiolated Graphene. *J. Phys. Chem. C* **2009**, *113*, 5612–5619.
23. Chua, C. K.; Pumera, M. Regeneration of a Conjugated sp^2 Graphene System through Selective Defunctionalization of Epoxides by Using a Proven Synthetic Chemistry Mechanism. *Chem.—Eur. J.* **2014**, *20*, 1871–1877.
24. Ferrari, A. C. Raman Spectroscopy of Graphene and Graphite: Disorder, Electron-Phonon Coupling, Doping and Non-adiabatic Effects. *Solid State Commun.* **2007**, *143*, 47–57.
25. Moon, I. K.; Lee, J.; Ruoff, R. S.; Lee, H. Reduced Graphene Oxide by Chemical Graphitization. *Nat. Commun.* **2010**, *1*, 73.
26. Wang, J.; Dai, J.; Yarlagadda, T. Carbon Nanotube-Conducting-Polymer Composite Nanowires. *Langmuir* **2005**, *21*, 9–12.
27. Ji, X.; Banks, C. E.; Crossley, A.; Compton, R. G. Oxygenated Edge Plane Sites Slow the Electron Transfer of the Ferro-/Ferricyanide Redox Couple at Graphite Electrodes. *ChemPhysChem* **2006**, *7*, 1337–1344.
28. Nicholson, R. S. Theory and Application of Cyclic Voltammetry for Measurement of Electrode Reaction Kinetics. *Anal. Chem.* **1965**, *37*, 1351–1355.
29. Wang, L.; Ambrosi, A.; Pumera, M. "Metal-Free" Catalytic Oxygen Reduction Reaction on Heteroatom-Doped Graphene Is Caused by Trace Metal Impurities. *Angew. Chem., Int. Ed.* **2013**, *52*, 13818–13821.
30. Cote, L. J.; Kim, F.; Huang, J. Langmuir-Blodgett Assembly of Graphite Oxide Single Layers. *J. Am. Chem. Soc.* **2009**, *131*, 1043–1049.